# The relation of the performance characteristics of pseudomorphic $In_{0.53+x}Ga_{0.47-x}As/In_{0.52}Al_{0.48}As$ ($0 \leqslant x \leqslant 0.32$) modulation-doped field-effect transistors to molecular-beam epitaxial growth modes

J. Pamulapati, R. Lai, G. I. Ng, Y. C. Chen, P. R. Berger, P. K. Bhattacharya, J. Singh, and D. Pavlidis
*Center for High-Frequency Microelectronics and Solid State Electronics Laboratory, Department of Electrical Engineering and Computer Science, The University of Michigan, Ann Arbor, Michigan 48109-2122*

(Received 31 January 1990; accepted for publication 13 March 1990)

We have examined the growth and device characteristics of $In_{0.53+x}Ga_{0.47-x}As/In_{0.52}Al_{0.48}As$ ($0 \leqslant x \leqslant 0.27$) pseudomorphic modulation-doped field-effect transistors on InP substrates. *In situ* reflection high energy electron diffraction oscillation studies were carried out to study the growth of pseudomorphic InGaAs on GaAs and InP substrates. The data from these measurements and a theoretical formalism based on energy minimization suggest that in the pseudomorphic growth regime increased strain causes growth modes to change from two-dimensional layer-by-layer to a three-dimensional island mode. The resulting interface roughness is used as a parameter to explain the observed trends in channel mobility and device performance. It is also shown that altered growth techniques, such as migration enhanced epitaxy, in which the surface reconstruction may be changed, can restore the layer-by-layer growth mode for large amounts of strain in the pseudomorphic layer.

## I. INTRODUCTION

There has been increased interest in the $In_{0.53}Ga_{0.47}As/In_{0.52}Al_{0.48}As$ heterostructure system, lattice matched to InP, for modulation-doped field-effect transistors (MODFET). This system is suited for use in microwave applications and is well suited for optoelectronic and communication applications in the 1.3–1.55 $\mu$m spectral range.[1-3] The InGaAs/InAlAs system on InP has two major advantages over GaAs-based MODFETs: (i) a greater conduction-band discontinuity ($\Delta E_c \sim 0.5$ eV) which results in greater confinement and higher sheet carrier densities, and (ii) a slightly lower electron effective mass in the channel leading to greater mobility. While inherently a better material system for MODFET applications, this heterostructure, however, has a ternary well causing increased alloy scattering in the channel. By the use of biaxial compressive strain in the channel region by increasing the In content in it, we can slightly reduce the electron effective mass and increase the confinement potential, as well as reduce the amount of alloy scattering.

Pseudomorphic epitaxy has increased the interest in basic material studies for the design devices such as MODFETs. Both *n*- and *p*-type pseudomorphic MODFETs have been reported with superior performance.[4-6] Although work has been done in the area of transport and device performance of these structures, little work has been done in the area of pseudomorphic growth and its relationship to devices. Since pseudomorphic devices involve thin quantum wells with thicknesses below critical thickness, it is important to understand the epitaxial growth modes, since interface roughness is controlled by growth modes. The interface roughness, in turn, controls mobility and eventually the performance of devices.[7,8] In this paper we will address the issue of both molecular beam epitaxial (MBE) growth modes and transport in pseudomorphic structures and their relation to MODFET device performance. Section II deals with growth modes under biaxial compressive strain. Section III deals with mobility and device performance of pseudomorphic *n*-type MODFETs. The results are discussed in Sec. IV and conclusions are made in Sec. V.

## II. THEORETICAL CONSIDERATIONS

In this section we will present the theoretical considerations on $In_xGa_{1-x}As$ on GaAs growth and focus on the pseudomorphic regime (i.e., InGaAs thickness below critical thickness[9]). Before discussing our results we briefly outline some important issues in epitaxy by techniques such as MBE. Since atoms and molecules (Ga, In, $As_4$) impinge randomly on the substrate, kinetics and thermodynamics both play important roles in establishing the growth modes. Thermodynamic parameters such as surface bond strengths and substrate temperature (free energy = internal energy $- T_{sub} \times$entropy) decide whether in equilibrium the surface is atomically abrupt or three-dimensional in nature. Kinetic parameters (surface migration and evaporation) decide whether or not the thermodynamic equilibrium state is reached. If the surface migration rate of the impinging atoms is high and thermodynamics favor an atomically abrupt surface, a layer-by-layer growth mode results. On the other hand if the surface kinetics are very small or the thermodynamics equilibrium state is not atomically flat, a three-dimensional growth mode will result.[10] These growth modes can be observed *in situ* by reflection high-energy electron diffraction (RHEED) oscillation studies.[11,12]

In the case of (100)-oriented growth, the energy difference between an atomically abrupt and a rough surface results from second-neighbor bond strengths under the appropriate surface reconstruction, as can be seen from Fig. 1.

 0021-8979/90/130347-04$03.00  

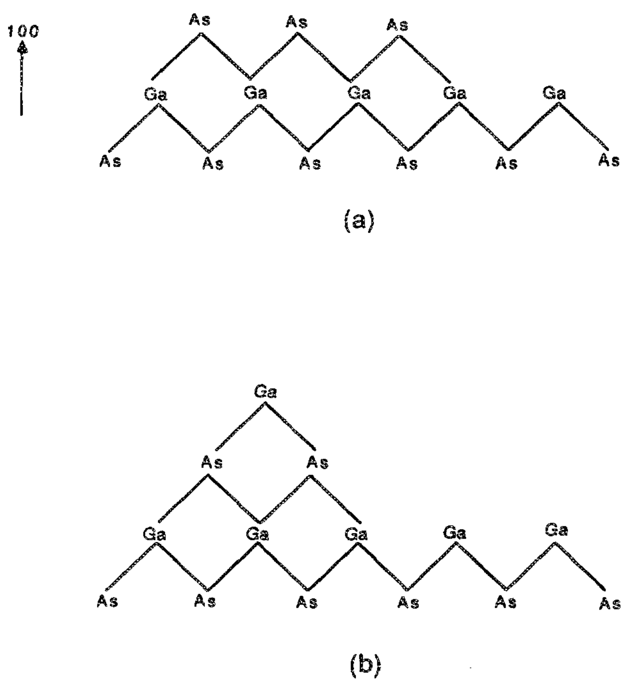


FIG. 1. (a) Atomically abrupt and (b) rough (100) surface. The atoms on the rough surface have the same number of nearest-neighbor bonds but fewer second-neighbor bonds.

Thus, in absence of biaxial strain, if the second neighbor bond energy $\omega_2$ is larger than $kT_{sub}$, the equilibrium state is atomically abrupt and a layer-by-layer growth mode can result if the surface kinetics are sufficiently high.[13] In Figs. 2(a) and 2(b) we show RHEED oscillations for the lattice matched growth of GaAs on GaAs and $In_{0.53}Ga_{0.47}As$ on InP. As can be seen from the sustained oscillations, layer-by-layer growth occurs.

In the case of the strained system, in addition to the second neighbor bond energy, $\omega_2$, one has to consider the strain energy in determining the thermodynamic equilibrium state. Using a simple model and energy minimization techniques we have shown[13] that the surface prefers to be formed from islands rather than have an atomically flat profile and that the height $n$ (in monolayers) of the islands is given by

$$n^3 \cong 2(\omega_1/\omega_2)(R_0/d_c), \tag{1}$$

where $\omega_1/\omega_2$ is the ratio of the nearest-to-second neighbor bond energies, $R_0$ is the substrate lattice constant, and $d_c/R_0$ is the height in monolayers of the critical thickness. At critical thickness the strain energy equals the dislocation formation energy. For lattice matched systems ($d_c \to \infty$), $n$ goes to zero, i.e., to an atomically flat surface. However, as the value of $d_c$ decreases (i.e., lattice mismatch increases) we expect a three-dimensional surface. In Figs. 2(c) and 2(d) we have shown RHEED oscillation data for growth of strained $In_{0.3}Ga_{0.7}As$ on GaAs and InGaAs on InP, respectively. As can be seen from this figure, in the presence of strain the layer grows in a three-dimensional (3D) mode which is reflected by the abrupt decay of the RHEED oscillations. In the next section we will discuss results on transport properties and performance characteristics of pseudomorphic $n$-type MODFETs and relate them to our observations on growth modes.

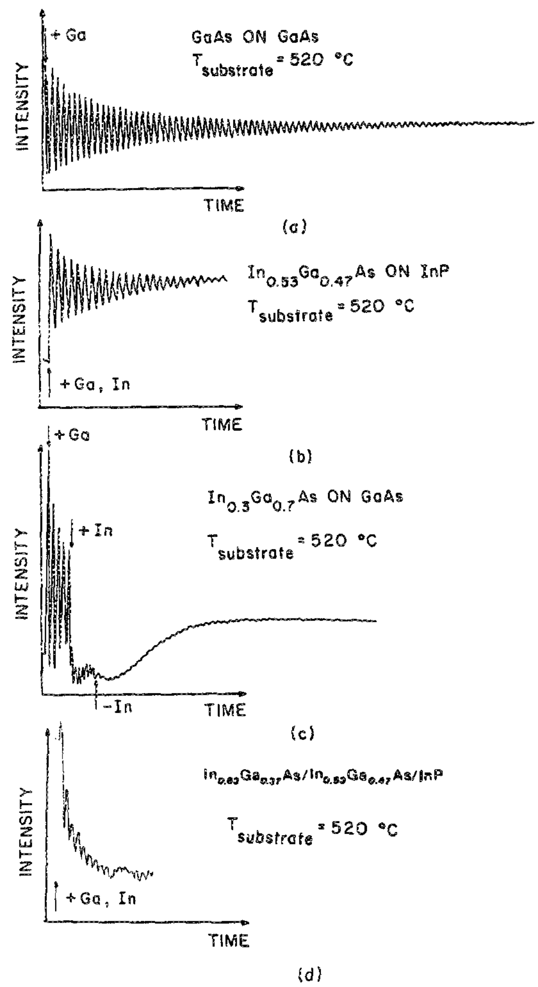


FIG. 2. RHEED oscillations data for MBE growth of (a) GaAs on GaAs, (b) $In_{0.53}Ga_{0.47}As$ on InP, (c) $In_{0.3}Ga_{0.7}As$ on GaAs, and (d) $In_{0.63}Ga_{0.37}As$ on InP.

## III. TRANSPORT PROPERTIES AND DEVICE PERFORMANCE

We have carried out experiments on both GaAs- and InP-based pseudomorphic MODFET heterostructures. We will discuss the results obtained from InP-based structures having a 40–150 Å, $In_{0.53+x}Ga_{0.47-x}As$ ($0 \leqslant x \leqslant 0.32$) quantum-well channel. The schematic of a typical structure grown by MBE is shown in Fig. 3. The growth conditions were optimized for growth as reflected in photoluminescence of single and multilayers as well as the mobility of bulk $In_{0.53}Ga_{0.47}As$ layers. The buffer for the samples was grown at $\sim 500$ °C. The growth was then interrupted to reduce the growth temperature and give sufficient time for the $In_{0.52}Al_{0.48}As$ buffer to become smooth. The channel consists of 400 Å of $In_{0.53}Ga_{0.47}As$ and 40–150 Å of $In_{0.53+x}Ga_{0.47-x}As$ for $0 \leqslant x \leqslant 0.32$. The reduced temperature was chosen not only for the bulk properties observed in our laboratory (for this temperature growth) but also to limit the thermodynamic parameters. The temperature was

| | | |
|---|---|---|
| 150 Å | $In_{0.53}Ga_{0.47}As$ | $n^+$ ($5\times10^{18}$ cm$^{-3}$) |
| 200 Å | $In_{0.52}Al_{0.48}As$ | i |
| 150 Å | $In_{0.52}Al_{0.48}As$ | $n^+$ ($5\times10^{18}$ cm$^{-3}$) |
| 50 Å | $In_{0.52}Al_{0.48}As$ | i |
| 100 Å | $In_xGa_{1-x}As$ | i |
| 400 Å | $In_{0.53}Ga_{0.47}As$ | i |
| 4000 Å | $In_{0.52}Al_{0.48}As$ | i |
| | InAlAs/InGaAs Superlattices | i |
| | S. I. InP (100) Substrate | |

FIG. 3. Schematic of MBE-grown $n$-type pseudomorphic MODFET on InP.

immediately increased for growth of the spacer layer and the donor layer. The inclusion of the intrinsic $In_{0.52}Al_{0.48}As$ is for device fabrication purposes. Finally, a heavily doped $In_{0.53}Ga_{0.47}As$ layer was grown to facilitate low-resistance ohmic contacts. The growth rate was fixed at 0.7 $\mu$m/h for both $In_{0.53}Ga_{0.47}As$ and $In_{0.52}Al_{0.48}As$. Hall measurements were made on van der Pauw samples to determine the transport properties. The sheet electron density in all the samples varied in the range $(2.0\text{–}3.2)\times10^{12}$ cm$^{-2}$. In Fig. 4 we show a plot of the 300 and 77 K mobilities versus excess In content in the channel. It may be noted that as excess In is added, initially the mobility increases as expected. However, upon further increase of In, the mobility starts to saturate.

MODFET transistors, with 0.7-$\mu$m gate stripes, were fabricated on the heterostructures by standard photolithography and liftoff techniques. Ge/Au/Ni/Ti/Au (700 Å/1400 Å/500 Å/200 Å/1000 Å) ohmic contacts were formed after a mesa isolation. Following a shallow recess a Ti/Au (500 Å/3000 Å) was evaporated for the gate stripes. Additional Ti/Au (1000 Å/10 000 Å) was evaporated for microwave characterization. A lower value of peak current was observed in some of the samples and was caused by a slight over-recess of those devices. All of the samples exhibited good pinch-off characteristics and low output conductances. Microwave measurements on the samples were done using a cascade probe station with a HP 8510B network analyzer. The devices were biased near their peak $g_m$ value. From the measured $S$ parameters, the extrinsic values of $f_T$ and $f_{max}$ were extrapolated. Table I shows the summary of the dc and microwave characteristics measured for each of the samples. The excellent dc and microwave results confirm the high quality of these layers.

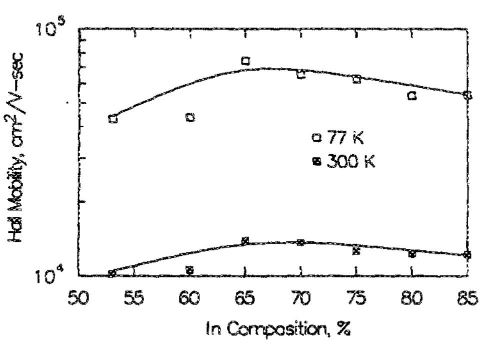


FIG. 4. Hall mobilities of pseudomorphic MODFET with increasing indium content in the channel at 77 and 300 K.

TABLE I. DC and microwave characteristics of $0.8\times150$ $\mu$m gate MODFETs with pseudomorphic $In_xGa_{1-x}As/In_{0.52}Al_{0.48}As$ quantum wells.

| $x$ | $g_{m,max}$ (mS/mm) | $I_{ds,max}$ (mA/mm) | $f_T$ (GHz) | $f_{max}$ (GHz) |
|---|---|---|---|---|
| 53 | 440 | 530 | 30 | 44 |
| 60 | 390 | 270 | 30 | 40 |
| 65 | 510 | 500 | 40 | 52 |
| 70 | 550 | 510 | 45 | 62 |
| 75 | 370 | 310 | 36 | 47 |
| 80 | 430 | 270 | 41 | 50 |
| 85 | 400 | 420 | 33 | 51 |

## IV. DISCUSSION

The trend in the mobility data as a function of In content observed by us—an initial increase followed by a decrease at higher values of strain (In content)—has been observed by other authors.[14] Since the carrier mass is not expected to show a turnaround, to explain the mobility data it is important to examine other scattering mechanisms. The dominant mechanisms which could explain the decreased mobility at higher In composition are interface roughness scattering and alloy scattering. For the GaAs-based structures, the alloy scattering continuously increases as In composition $x$ is increased [since $\mu\propto 1/x^2(1-x)^2$]. However, for the InP-based systems the alloy scattering should decrease since the alloy scattering peaks for a 50:50 alloy, assuming the mass does not vary. Thus, unless some unusual clustering effects occur in strained epitaxy, one has to consider interface roughness as the source of the turnaround in mobility as the excess In composition increases beyond $\sim15\%$. The interface roughness scattering can be described by the scattering time,[8]

$$\frac{1}{\tau}=\frac{\pi e^4 m^*}{\hbar^3\epsilon_s^2}N_s^2\Delta^2\int_0^\pi J_1(k_F L\sin\phi)^2 d\phi, \tag{2}$$

where $N_s$ is the sheet charge density, $\Delta$ is the height of the 3D island describing the interface roughness, $L$ is the lateral extent of the island, and $k_F$ is the Fermi vector. From the discussion in Sec. II we expect $\Delta$ to abruptly increase when the strain increases to $\sim2\%$. We expect that if $\Delta$ increases to $\sim4$ monolayers around this value of strain, the mobility decreases at high In content can be accounted for. The RHEED data of Figs. 2(c) and 2(d) suggest that this is quite likely the case. The device dc and microwave characteristics also show an initial rapid improvement with increasing In content in the channel up to $x=0.65$, after which there is only marginal improvement. We believe that the reasons are the same as that attributed for the mobility trend.

Since the minimum free energy for a strained system favors a 3D surface, the growth of strained systems cannot be improved by simply enhancing the surface migration rate of the adatoms. One expects the free energy to depend upon the surface reconstruction during growth. In MBE the surface is anion stabilized with a $c(2\times4)$ reconstruction. It is therefore important to examine other possible surface reconstructions which might change the surface chemical energy. Since MBE of III-V semiconductors cannot be carried out under cation rich condition because the excess cation causes nonstoichiometric growth, a viable approach is migration-enhanced epitaxy (MEE),[15-18] where a few monolayers (up to 4) of cations and a few monolayers of the anion are alternately deposited by shutter control. The surface recombination thus alternates between cation and anion stabilized. We have therefore made RHEED oscillation measurements during the growth of $In_xGa_{1-x}As$ on GaAs ($x = 0.2$ and 0.3) under MEE growth conditions. A GaAs buffer layer is first grown by MBE at 1 $\mu$m/h. Strained InGaAs is then grown by MEE at ~600 °C at a rate of 0.6 $\mu$m/h. Shown in Fig. 5 are the observed RHEED oscillations for growth of $In_{0.1}Ga_{0.9}As$ and $In_{0.2}Ga_{0.8}As$.

During MEE growth the surface changes from cation stabilized to anion stabilized phase alternatively, corresponding to the opening of the source shutters. This makes the structure of the oscillations very different from those of the anion stabilized MBE case. If the shutter opening time is properly adjusted, a complete recovery of the smoothness of the growth front is possible, with long-lasting oscillations. Differences in RHEED patterns between MBE and MEE are also observed for $In_xGa_{1-x}As$ with $x = 0.3$. In MBE growth, the RHEED pattern becomes spotty after a few monolayers are deposited. In MEE, the pattern remains streaked even after 20 monolayers, suggesting the growth is perfectly two dimensional.

## V. CONCLUSIONS

In conclusion, we have addressed the issue of growth modes in MBE-grown strained layers in the context of the performance characteristics and transport properties of InP-based pseudomorphic MODFETs. It is observed that the mobility increases as excess In is added in the channel layer, but starts decreasing above ~20% excess indium. The dc and microwave characteristics also show a saturating trend after an initial rapid improvement. We have related these trends to the MBE growth modes of strained layers. From RHEED oscillation measurements and energy minimization considerations it is apparent that once the misfit strain in the InGaAs channel increases above ~1.5%–2.0%, the growth occurs in a 3D island mode, leading to a rough interface. The change in the growth mode occurs because of the competition between surface strain energy and the second neighbor bond strength. We note that the second-neighbor bond strengths may be different for different surface reconstruction so that it may be possible to grow layer-by-layer even at high strain under some reconstruction. An example, as shown here, is the case of migration enhanced epitaxy, in which alternate monolayers are grown under Gr. III and Gr. V stabilized conditions. RHEED oscillation data suggest that indeed a layer-by-layer growth mode is maintained even for high strain values.

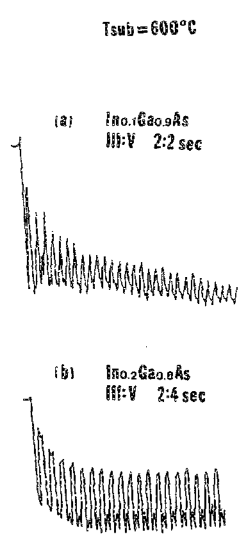


FIG. 5. RHEED intensity oscillations observed during growth of $In_xGa_{1-x}As$ by MEE at 600 °C. (a) $P_{Ga} = 4.65\times10^{-7}$ Torr, $P_{In} = 1.02\times10^{-7}$ Torr, (b) $P_{In} = 2.05\times10^{-7}$ Torr.

## ACKNOWLEDGMENTS

This work was supported by the Office of Naval Research under Contract No. N00014-89-J1519 and the Army Research Office (URI Program) under Contract No. DAAL03-87-K-0007.

[1]U. K. Mishra A. S. Brown, and S. E. Rosenbaum, *IEDM Technical Digest* (IEEE, New York, 1988) p. 180.
[2]P. C. Chao, A. J. Tessmer, K-H. G. Duh, P. Ho, M.-Y. Kao, P. M. Smith, J. M. Ballingall, S.-M. J. Liu, and A. A. Jabra, Electron. Dev. Lett. **11**, 59 (1990).
[3]Y. Zebda, P. K. Bhattacharya, D. Pavlidis, and J. Harrang, J. Appl. Phys. (to be published).
[4]G. I. Ng, W.-P. Hong, D. Pavlidis, M. Tutt, and P. K. Bhattacharya, Electron. Dev. Lett. **9**, 439 (1988).
[5]U. K. Mishra, A. S. Brown, S. E. Rosenbaum, C. E. Hooper, M. W. Pierce, M. J. Delaney, S. Vaughn, and K. White, Electron. Dev. Lett. **9**, 647 (1988).
[6]T. J. Drummond, T. E. Zipperian, I. J. Fritz, J. E. Schirber, and T. A. Plut, Appl. Phys. Lett. **49**, 461 (1986).
[7]T. Ando, J. Phys. Soc. Jpn. **51**, 3900 (1981).
[8]W.-P. Hong, J. Singh, and P.K. Bhattacharya, Electron. Dev. Lett. **7**, 480 (1986).
[9]J. W. Matthews and A. E. Blakeslee, J. Cryst. Growth **27**, 118 (1974).
[10]J. Singh and K. K. Bajaj, Superlattices and Microstructures **2**, 185 (1986).
[11]J. H. Neave, P. J. Dobson, B. A. Joyce, and J. Zheng, Appl. Phys. Lett. **47**, 100 (1985).
[12]J. M. Van Hove, P. R. Pukite, G. J. Whaley, A. M. Wouchak, and P. I. Cohen, J. Vac. Sci. Technol. B **3**, 1116 (1985).
[13]P. R. Berger, K. Chang, P. K. Bhattacharya, J. Singh, and K. K. Bajaj, Appl. Phys. Lett. **53**, 684 (1988).
[14]C. K. Peng, S. Sinha, and H. Morkoç, J. Appl. Phys. **62**, 2880 (1987).
[15]J. M. Gerard and J. Y. Marzin, Appl. Phys. Lett. **53**, 568 (1988).
[16]R. Katsumi, H. Ohno, H. Ishii, K. Matsuzaki, Y. Akatsu, and H. Hasegawa J. Vac. Sci. Technol. B **6**, 593 (1988).
[17]J. M. Gerard, J. Y. Marzin, B. Jusserand, F. Glas, and J. Primot, Appl. Phys. Lett. **54**, 30 (1989).
[18]L. Gonzales, A. Ruiz, A. Mazuelas, G. Armelles, M. Recio, and F. Briones, Superlattices and Microstructures **5**, 5 (1989).